Structure, Optical, Corrosion, and Photocatalytic Properties of Thermally Evaporated Molybdenum Trioxide Thin Films Deposited on Different Substrates

Sh. A. Elkot[1]*, W. S. Mohamed*[1, 2]*, Mahmoud Elrouby*[3]*, H. M. Ali* [*1] *and E. Kh. Shokr*[1]

[1]Physics Department, Faculty of Science, Sohag University, 82524 Sohag, Egypt.
[2]Physics Department, College of Science, Jouf University, Al-Jouf, Sakaka, P.O. Box 2014, Saudi Arabia.
[3]Chemistry Department, Faculty of Science, Sohag University, 82524 Sohag, Egypt.

Abstract: In this study, we report the physical properties of sub-stoichiometric Molybdenum trioxide (MoO_{3-x}) thin films synthesized by thermal evaporation technique for photocatalytic application. MoO_{3-x} thin films were deposited on glass and Fluorine doped Tin Oxide (FTO) coated glass substrates with different thicknesses (100 - 650 nm). Structure analysis by X-ray diffraction and field emission scanning electron microscope confirm the amorphous structure of MoO_{3-x} films deposited on FTO and glass substrates. The optical analysis by UV-Vis–near-infrared spectrophotometer showed that the optical band gap does not depend on the substrate type and takes values in the range from 3.6 to 3.31 eV. The Corrosion measurements for MoO_{3-x} films deposited on FTO coated glass substrates were performed using an electrochemical potentiostat in a neutral medium of NaCl solution. The corrosion studies demonstrate that the as deposited MoO_{3-x} film of thickness 650 nm exhibits the highest corrosion resistivity compared with other thicknesses. The methylene blue (MB) was employed as a representative dye pollutant to evaluate the photocatalytic activity of the current samples. The results show that the film thickness and substrate type play an important role in the enhancement of the photocatalytic properties of MoO_{3-x} films. We found that the deposited films on glass decompose MB more than the films deposited on FTO. In addition, the as deposited MoO_{3-x} film of thickness 100 nm exhibit the highest photocatalytic activity as compared with the other deposited films.

Keywords: MoO_{3-x} thin films; thermal evaporation; x-ray diffraction; optical analysis; corrosion; photocatalytic activity.

1 Introduction

Molybdenum trioxide (MoO_{3-x}) is one of the most important transition metal oxide materials by the virtue of its high stability. In the last few years huge efforts were dedicated to exploit the optical and electrical properties of MoO_{3-x} thin films in many different industrial applications [1,2] such as catalysts, photoluminescence, photovoltaics, photochromisms, electrochromisms, sensors, and batteries [2-4]. On the other hand, various techniques were used to synthesis oxide materials, such as thermal evaporation [2, 5, 6] chemical vapor deposition [7], electrodeposition [8] spray pyrolysis [9], sol gel [10, 11] and DC magnetron sputtering [12, 13]. In this work, the thermal evaporation is selected to prepare MoO_{3-x} thin films with different thickness because this process leads to a careful control of the film thickness, also MoO_{3-x} thin films can be easily prepared by using many and different evaporation techniques [1].the usage of thermal evaporation techniques for depositing thin films from oxide materials with relatively high oxygen index such as MoO_3, WO_3 and V_2O_5 produces n or p- type thin films according to the deposition conditions [2,3,14]. This qualifies the deposited films to be used in many applications. One of them is a photocatalyst that accelerates chemical reactions. A number of researchers have studied TiO and ZnO as a photocatalyst [15-19]. Mai M. Khalaf et al studied TiO thin films doped with Co to be used as a photocatalyst for water purification from organic pollutants [15]. Phutthamon Chantes et al studied the ability of TiO_2 and ZnO to be used as a photocatalyst on the Degradation of Real Batik Wastewater

---

[*]Corresponding author e-mail: hazem95@yahoo.com

[16]. Others have studied MoO_3 to be used in the photocatalysis and photovoltaic applications [20-25].

It's important to study how much the as-deposited MoO_{3-x} can be corroded to know the optimum thickness corresponding to the highest corrosion resistivity. Many corrosion phenomena are occurring due to the electrochemical reaction. Hence, their study required different techniques to be accurately detected. Electrochemical technique for the measurement of corrosion is considered as the optimum method for corrosion detection due to its speed [26], affectivity and accuracy for metals or alloys that have high corrosion resistant with respect to many other methods such as weight loss method. Electrochemical technique can be used to give important information about the specimen such as corrosion rates, coatings, films passivity, pitting tendencies and many other important data [26,27]. All of this important information can be easily obtained from the current-potential relation under carefully controlled conditions.

This paper studies the structural, surface topography, compositional, optical properties and corrosion for different thickness (100,200,300,500 and 650 nm) of the as deposited MoO_{3-x} thin film on glass and fluorine doped tin oxide coated glass (FTO) prepared by thermal evaporation technique. The validity of these films to be used as a photocatalyst for water purification from organic pollutants such as Methyl blue (MB) has been tested too.

2 Experimental Procedures

MoO_{3-x} thin films with different thicknesses (100, 200, 300, 500, 650 nm) have been deposited by thermal evaporation technique from a single source using a coating unit (Manufactured using Technology Licensed from Edwards Ltd, Auto 306, 2014).
MoO_3 powder provided by Aldrich with 99.999 % purity was cold pressed to be in a tablet form and placed in a molybdenum boat (melting point 2620 °C). This compressed tablet MoO_3 was used to prepare MoO_3 thin films on ultrasonically cleaned microscopic glass and fluorine doped tin oxide (FTO) coated glass. Substrates were cleaned rinsing by means of heated ultrasonic cleaner instrument (VGT-1613 QTD) provided with digital timer of capacity 2000 mL using both acetone and distilled water. Before deposition the chamber was evacuated to base vacuum of 4×10^{-4} mbar and the vacuum in end of deposition process was 3.63×10^{-5} mbar.

The film thickness and the deposition rate were monitoring by means of a digital film thickness monitor model INFICON (SQM-160). The deposition rate was in the range from 1 to 3 A°/sec.

X-ray diffraction (XRD) examination was used for examining the crystallographic structure of the as deposited films on glass, and FTO. In this work the (XRD) examination have been carried out using X-ray diffractometer type Philips (model PW1710, Netherlands) with Cu as target and Ni as filter, $\lambda=1.541838A^0$. The x-ray diffractometer work at 40 KV and 30 mA with a scanning speed 2^0/min. The diffraction scan was in the range (2θ) from 10 to 100°.

The surface topography and the compositional contents of some deposited MoO_{3-x} thin films on glass and FTO (thickness 200 and 500) have been checked by field-emission scanning electron microscopy (FE-SEM) using a JSM-6100 microscope (JEOL, Japan) with an acceleration voltage of 30KV. The chemical composition of the films was also analyzed using energy dispersive analysis of X-ray (EDAX) unit attached with the FE-SEM (EDS unit, HNU-5000, USA). Very thin layer of gold ~10 nm thick has been deposited over the samples before examination.

The optical properties (absorption A) were measured for as deposited films on glass and FTO at room temperature using a computer-programmable Jasco V570 (Japan) double beam spectrophotometer. The wavelength range was from 200 to 2500 nm at normal incidence with a scan speed of 400 nm/ min.

The optical measurements were used to determine several optical constants of the deposited MoO_{3-x} films, such as the absorption coefficient (α), the optical band gap energy Eg, the extinction coefficient (k) and refractive index (n).

Corrosion measurements for MoO_3-x films deposited on FTO coated glass substrates were performed for films of 100, 200, 300, 500 and 650 nm thick using an electrochemical potentiostat VersaSTAT 4. A glass three-electrode electrochemical cell has been used. The deposited films used as a working electrode (WE), the counter electrode (CE) are a rod of Platinum (Pt) and the reference electrode (RE) is silver chloride (Ag/AgCl). The VersaSTAT 4 controls the potential at the working-sense electrode with respect to the reference electrode. In this work, the three electrodes WE, CE and RE were immersed in 3.5g/ml NaCl as a supporting electrolyte solution and the range over which the working electrode potential controlled is ± 250 mV. Fig.1 illustrates simple design for the electrochemical potentiostat circuit which has been used to study the corrosion through the occurred electrochemical reactions [28].

The as deposited MoO_{3-x} films on glass and FTO have been tested to be used as a photocatalyst for water purification from organic pollutants such as Methyl blue (MB) .This can be performed by immersing these films in .001g/ml Methyl blue (MB) solution for one hour, extract theme out of the solution and let them to dry in dark for one hour. Transmittance was measured for the films before and after the exposure to UV irradiation for each five mints until the total irradiation time reaches to two hours. Using the value of transmittance at 580 nm before illumination T_0 and after illumination Ti (after each 5 min), the change of absorbance ΔABS characterizing the decomposition of MB has been calculated as ΔABS =ln (T_o/T_i). The illumination has been carried out using an UV light lamp (model ENF-240C/FE) with a wavelength of 254 nm.

3 Results and Discussion

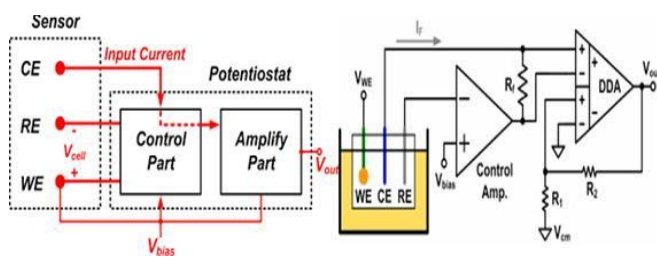Figure 2 shows the X-ray diffraction (XRD) patterns of the

Fig.1: Simple design for electrochemical potentiostat circuit.

as-deposited molybdenum oxide thin film on glass and fluorine doped tin oxide (FTO) coated glass substrates. For the as deposited films on glass, it's clear from Fig. (2, a) that the deposited films have amorphous structure since no diffraction peaks could be observed. This amorphous phase could have resulted from the interstitial or substituting location [2].

The XRD spectra for FTO substrate before and after the films deposition is presented in Fig. (2, b). The results of XRD suggest that the films have polycrystalline structure and all observed diffraction peaks belongs to the (FTO) coated glass substrate according to the (JCPDS No.41-1445) card, confirming the amorphous structure of MoO_{3-x} films on FTO. This amorphinity may be due to the dislocations and defects within the deposited films that leading to the complex structure of the energy states within the films.

Figure 3 depicts the SEM micrographs for as deposited MoO3-x thin films with 200 and 500 nm thick deposited on glass and FTO coated glass substrates. For MoO_{3-x} thin films deposited on glass with thickness 200 nm some nano spheres were observed and disappear by increasing the film thickness for film with 500 nm thick as in Fig (3,a, b). Some cracks were appeared in film with 200 nm thick, referring to high adhesion of film on the glass substrate. For MoO_{3-x} thin films deposited on FTO as in Figs. (3-c, d), the film has a compact and dense homogenous surface with cluster of spheres appear on it. The MoO3-x film with 500 nm thick shows some spherical grains with size lying in 100–200 nm. The orientation of these grain are randomly, some whole grains do not share a common border and so are surrounded by empty spaces. Finally in general, the SEM analysis shows that, by increasing the deposited film thickness the grain size increase.

Figure 4 indicates the EDAX spectrum of as deposited MoO_{3-x} thin films of 500 nm thick on FTO. It is observed that, there is an excess of Mo^{+5} atoms that work as point defects (impurity atoms) due to the deficiency of oxygen atoms (vacancy defects) in the deposited samples. The appeared Sn and Si in the EDAX spectrum come from the substrate components.

The optical absorption spectra of as deposited MoO_{3-x} films on glass and FTO coated glass are shown in **Fig.5.** It is observed that the absorption increases with increasing the film thickness as expected since the presence of oxygen
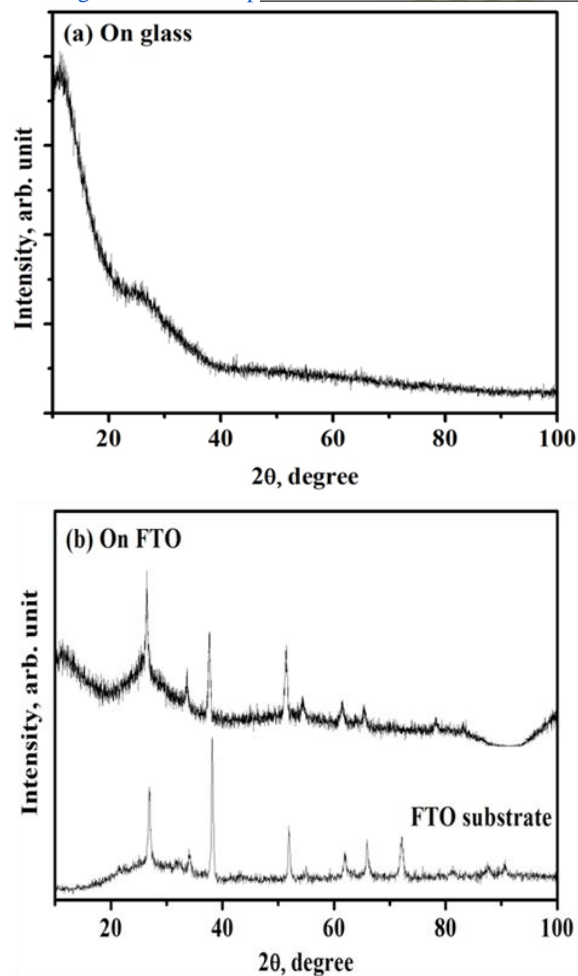

Fig.2: X-ray diffractograms of as-deposited molybdenum oxide thin films on (a) glass, (b) FTO.

vacancies can lead to the increase of the carrier concentration as the film thickness increments [7, 29, 30].

As shown in Fig. (5, a), the absorption of the deposited films on glass is very low in the near infrared region (NIR) compared with that for MoO_{3-x} films deposited on FTO. This may be due to the plasmonic reflection resulting by the relatively higher free carrier concentration of FTO substrate. For both MoO_{3-x} films either deposited on glass or FTO substrates, a high absorption values in both UV and visible regions can be depicted as shown in **Fig. (5 a, b)**.

The optical energy gab E_g has been calculated for both MoO_{3-x} films either deposited on glass or FTO substrates. It's observed that the substrate type doesn't have a sensitive effect on the optical band gap energy values, which agree with the matching in the absorption spectra in both UV and

visible regions for both MoO_{3-x} films either deposited on glass or FTO substrate. The calculated E_g values were matching with E_g values which have been measured in

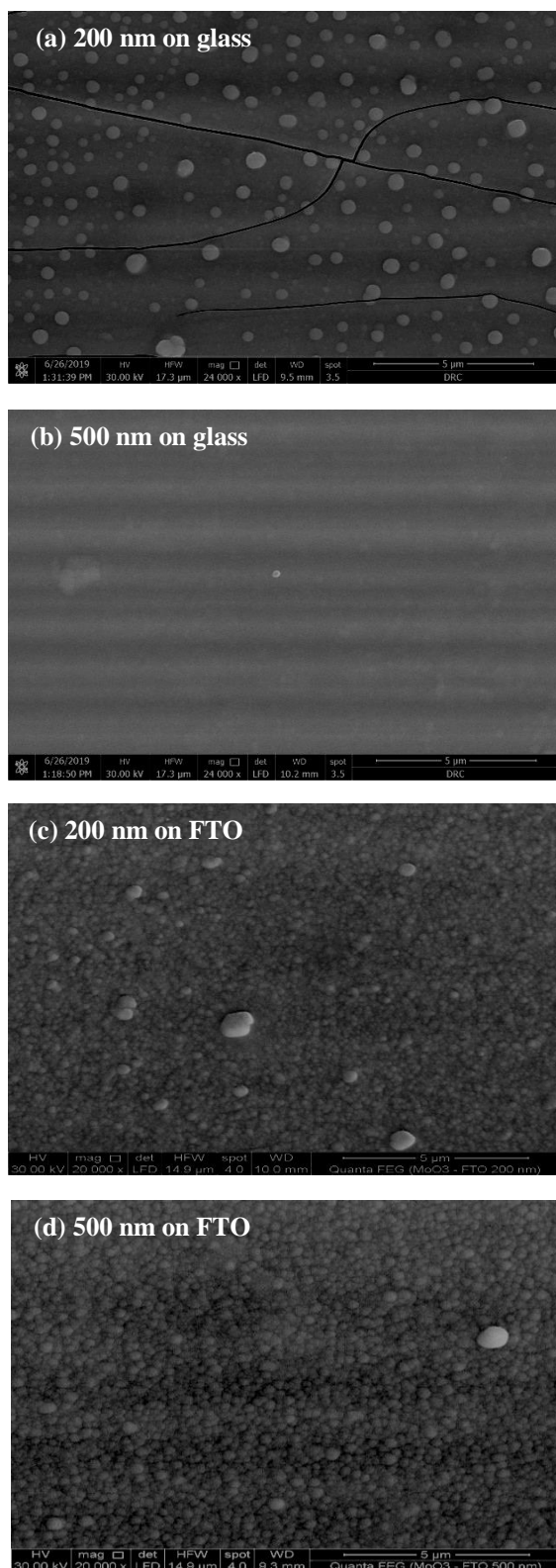many previous studies [2, 31, 32]. The E_g values are listed in Table 1.

Fig .3: SEM micrographs of as deposited MoO$_{3-x}$ thin films (a, c) on glass of 200 and 500 nm thick respectively and (b, d) on FTO of 200, 500 nm thikc respectively.
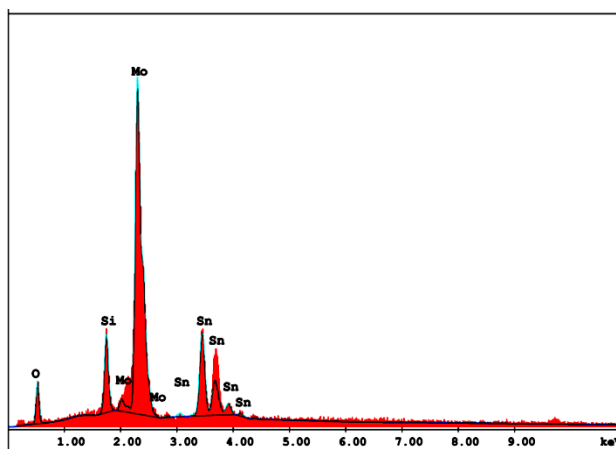

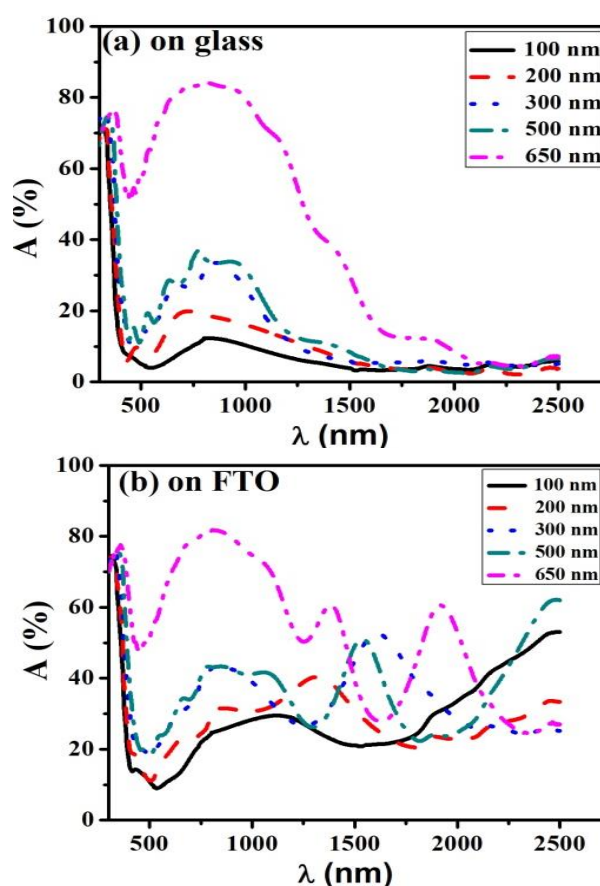**Fig. 4:** EDAX spectrum of as deposited MoO3-x thin films on FTO with thickness of 500 nm .

Fig.5: The optical absorbance spectra for the as deposited MoO3-x thin films (a) on glass and (b) FTO.

The absorption or the optical density near the absorption band edge is an exponential function of the photon energy as described by the Urbach law [33, 34].

$$\alpha = \alpha_0 \exp (h\upsilon/E_u) \qquad (1)$$

where, α_0 is a constant and E_U is the Urbach energy that gives the width of the tails of localized states in the gab

region [35]. E_u was determined from the slope of the straight line of Ln (α) vs. hυ relation and reported in Table 1. As shown, E_u decreases by increasing thickness for both films deposited on glass and FTO substrates.

The refractive index (n) and the extinction coefficient (k) of the as deposited MoO_{3-x} thin films of thickness (100,200,300,500 and 650nm) on glass and FTO substrates can be calculated by using the absolute values of the measured transmittance (T) and reflectance (R) according to Eqs. 2 and 3 as follows [36]

$$n = \frac{1+R^{1/2}}{1-R^{1/2}} \qquad (2)$$

$$k = \frac{\alpha \lambda}{4 \pi} \qquad (3)$$

Figure 6 depicts the wavelength dependence of refractive index (n) for MoO_{3-x} thin films deposited on (a) glass, (b) FTO substrates. The inset of Fig.5 refers to the variation of refractive index at wavelength equals to 550 nm with the thickness of the deposited film.

For as deposited MoO_{3-x} films on FTO substrate the refractive index is relatively high in the NIR region. This behavior may refer to the high carriers' concentration in films. By contrast, for MoO_{3-x} films deposited on glass, n values in NIR are relatively low. Also, both MoO_{3-x} films deposited on glass and FTO have the same average values of refractive index in the visible region (about 2.5), as reported in Table .1. As depicted in Fig.6, refractive index decreases with the increment of the as deposited film thickness at wavelength 550 nm for the as deposited films on glass and FTO substrates.

Figure 7, depicts the wavelength dependence of extinction coefficient (k) for MoO_{3-x} thin films deposited on (a) glass,

(b) FTO substrates respectively. It's observed that the extinction coefficient (k) for the as deposited films on FTO substrate in the NIR region is larger than that of the as deposited films on glass which again refers to higher carrier concentration in the former films than that in glass-

substrate films. The extinction coefficient (k) for MoO_{3-x} thin films deposited on (a) glass and FTO substrates

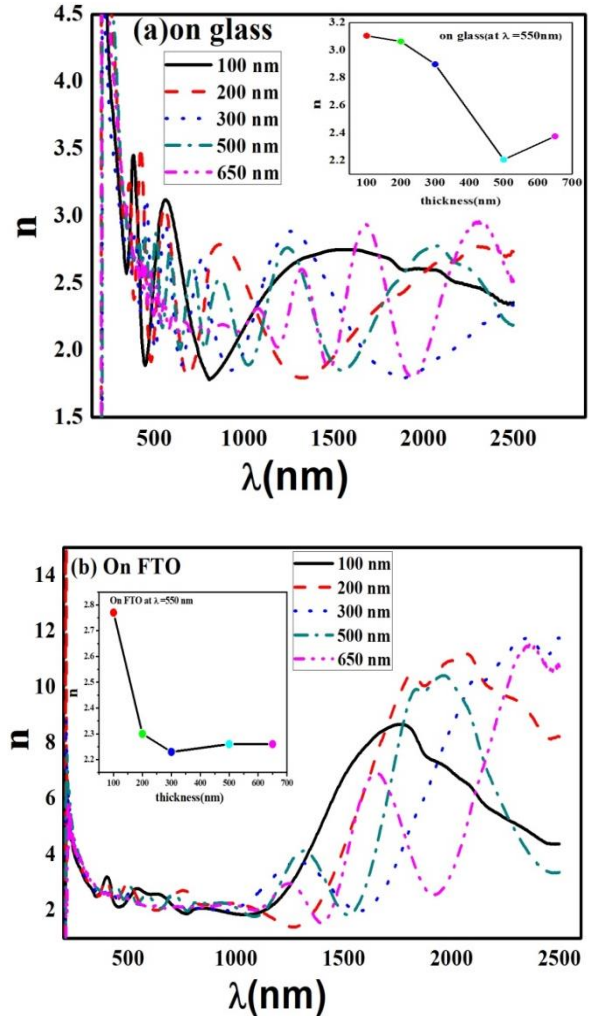increases with the film thickness increment as depicted in Fig. (7-c).

Fig.6: The wavelength dependence of refractive index (n) for MoO3-x thin films deposited on (a) glass, (b) FTO. The inset figure refers to the refractive index of the deposited film at wavelength equals to 550nm as a function of film thickness.

Table 1: includes E_g, n in the visible region, Urbach energy E_u , E_0 and E_d for MoO_{3-x} thin films deposited on both glass and FTO.

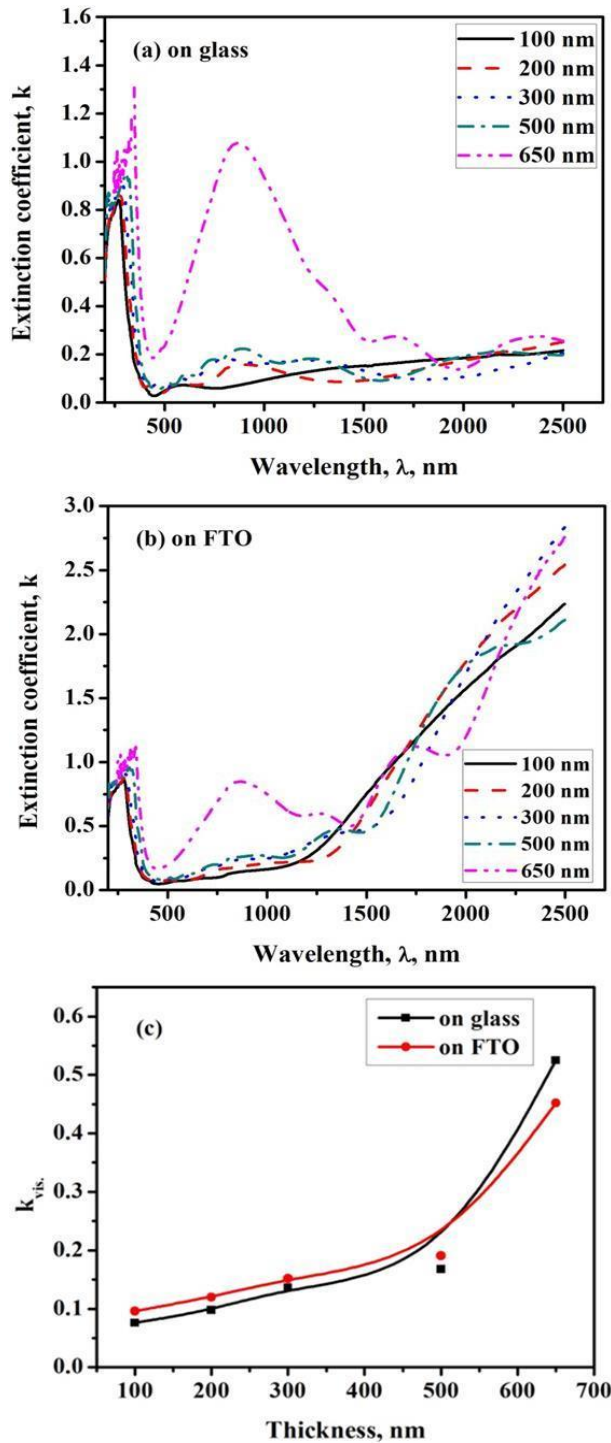| Thickness (nm)	deposited films on glass					deposited films on FTO				
	E_g (ev)	n average (320-800nm)	E_u (ev)	E_0 (ev)	E_d (ev)	E_g (ev)	n average (320-800nm)	Eu(ev)	E_0 (ev)	E_d (ev)
100	3.59	2.54	0.411	0.86	6.43	3.61	2.45	0.467	1.28	6.05
200	3.51	2.49	0.346	1.05	6.42	3.52	2.50	0.427	1.20	5.99
300	3.42	2.50	0.312	0.78	6.35	3.43	2.38	0.372	1.19	5.94
500	3.24	2.51	0.282	1.19	6.61	3.25	2.48	0.329	1.04	5.94
650	3.13	2.39	0.272	0.73	6.28	3.16	2.33	0.324	0.99	6.36

Fig.7: The wavelength dependence of extinction coefficient (k) for MoO_{3-x} thin films deposited on (a) glass,(b) FTO ,Fig (c) shows the variations in the visible region with the thickness of the as deposited film on glass and FTO.

The concept of single oscillator energy has been used to study and determine the optical dispersion parameters (Wemple, 1977; Di Domenico, 1972) [37, 38]. Below the interband absorption edge in the region of low absorption the refractive index could be expressed by the following relation;

$$\left(n^2 - 1\right)^{-1} = \frac{E_o}{E_d} - \frac{1}{E_o E_d}\left(h\nu\right)^2 \qquad (4)$$

Where, $h\nu$ is the photon energy, E_d is the electronic dispersion energy that represents the average strength of the optical inter band transitions and independent on either the band gap or the volume density of the electrons in the valence band and E_0 is the single oscillator energy which represents the mean transition energy from the valence band to the conduction state (Bakr et al, 2003). E_0 involves all the electronic transitions not only the transition from the top of the valence band to the bottom of the conduction band as in the optical band gap Eg. The relation between E_0 and E_g was found to be $E_0 \approx 0.3 E_g$ for the as deposited MoO_{3-x} films on glass and $E_0 \approx 0.35 E_g$ for MoO_{3-x} films on FTO. By plotting $(n^2-1)^{-1}$ against $(h\nu)^2$ and fitting a straight line, E_d and E_o can be determined directly from the slope $(E_d E_o)^{-1}$ and the intercept E_o/E_d on the vertical axis as shown in Fig.8 and listed in Table.1.
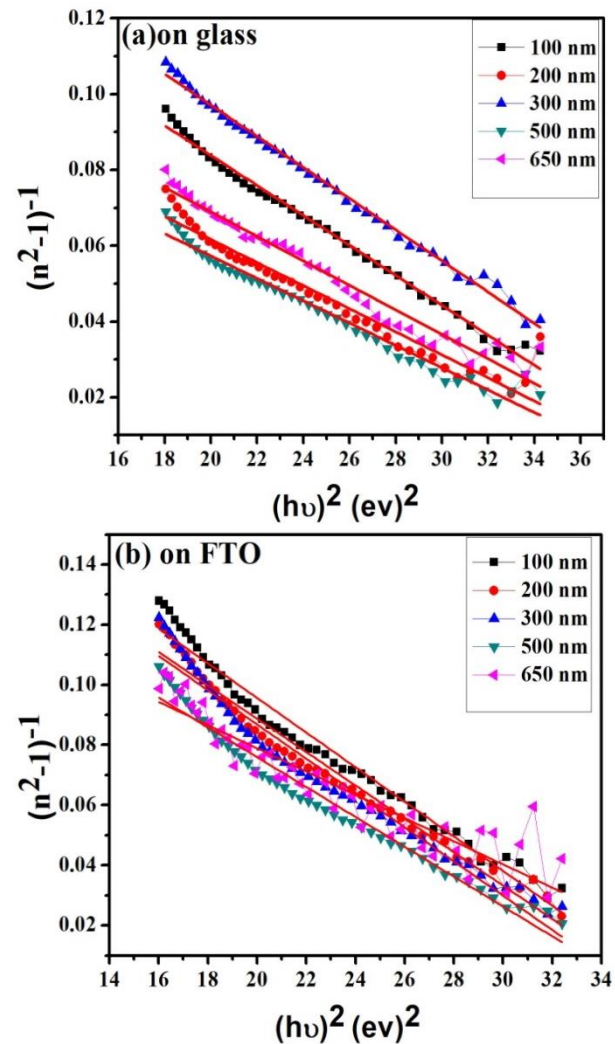

Fig.8: Plots of $(n^2-1)^{-1}$ versus $(h\nu)^2$ for MoO_{3-x} thin films with different thicknesses (a) on glass and (b) on FTO.
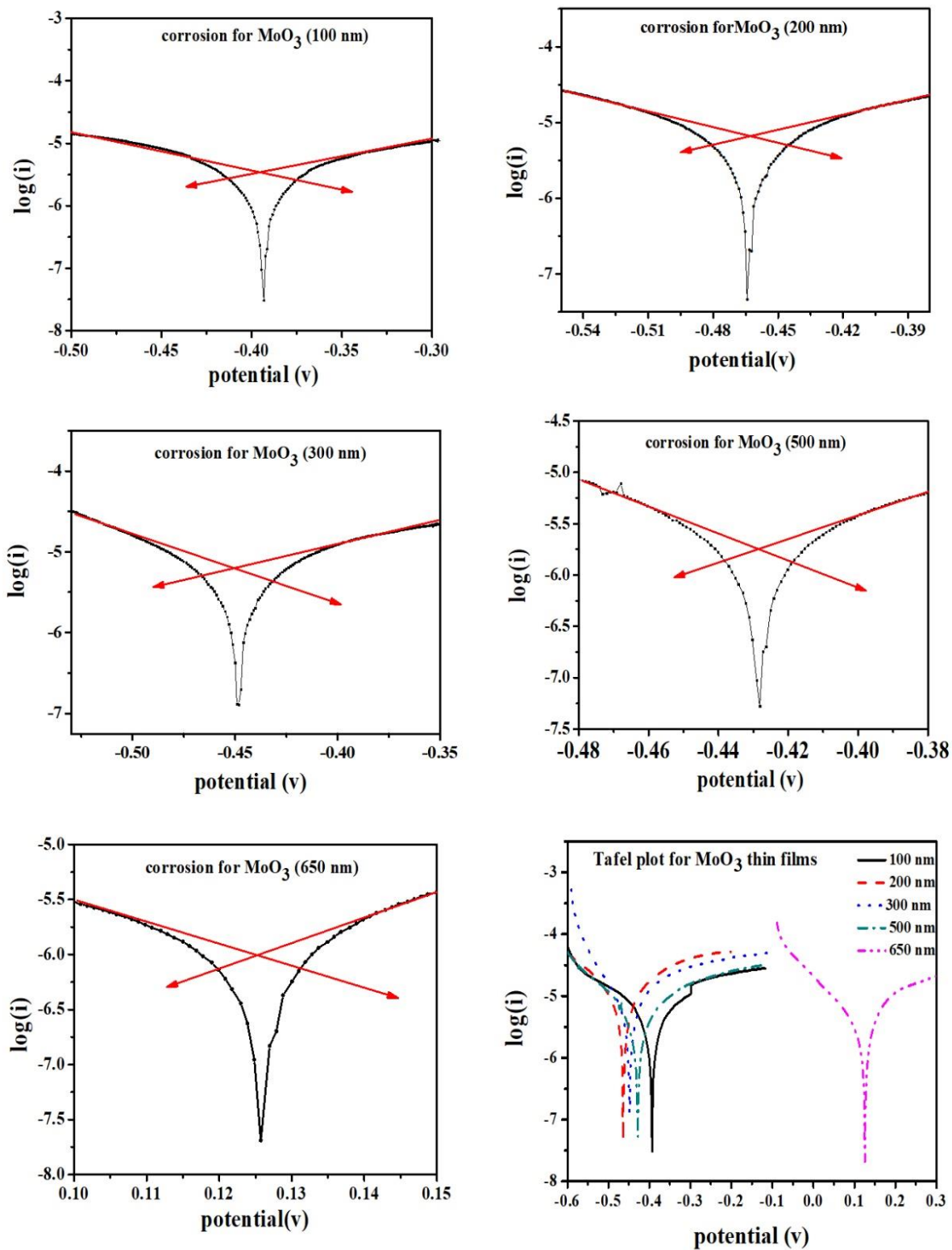
Fig.9: log (i) versus the applied potential for MoO$_{3-x}$ thin films of different thicknesses (100,200,300,500nm)deposited on FTO.

Tafel plot were performed for MoO_{3-x} thin films deposited on conductive FTO substrates by polarizing the specimen about 250 mV anodically (positive-going potential) and cathodically (negative-going potential) from the corrosion potential, E_{corr} (versus open circuit potential). The resulted current was plotted on a logarithmic scale versus the applied potential as shown in Fig. 9.

Tafel equation employed to study the corrosion phenomenon could be expressed as follows [27];

$$\eta = \beta \log \frac{i}{icorr} \qquad (5)$$

Where, β is Tafel constant, η is the over voltage, which is the difference between the potential imposed on the specimen and the corrosion potential and i_{corr} is the corrosion current at the over voltage and can be obtained from Tafel plot by extrapolating the linear portion of the curve to the value of E_{corr} [27] as depicted in Fig.9. By rearranging Eq. 5 one obtains;

$$\eta = \beta (logI - log\ i_{corr}) \qquad (6)$$

As shown in Fig. (10, a), i_{corr} decreases by increasing the film thickness from 100 nm up to 650 nm. This can be attributed to that the FTO substrate electrode becomes more fully covered with MoO_{3-x} layers by increasing the deposited film thickness making the deposited particles to be strongly stacked to the FTO substrate. So, MoO_{3-x} films of thickness 650nm are more protected films from corrosion as depicted in Fig. (10, a). It is also observed that the E_{corr} values increases by increasing the deposited film thickness as depicted in Fig. (10, b), this may be due to the variation of the surface structure morphology of the deposited films. This leads to the variation of the open circuit potential of the deposited films of different thicknesses.

The as deposited MoO_{3-x} films on glass and FTO substrates have been tested to be used as a photocatalyst for water purification from organic pollutants such as Methyl blue (MB). The photocatalyst coupled with UV lights can oxidize organic pollutants into nontoxic materials, such as CO_2 and water and can disinfect certain bacteria. Figs. (11 and 12) depict the transmittance spectra for the as-deposited MoO_{3-x} thin film deposited on glass and FTO substrates respectively. The transmittance spectra were measured for the 100, 200, 300 and 500 nm of film thickness before and after the exposure to UV irradiation for each five mints until the total irradiation time reaches two hours.

Figure 13 shows the variation of absorption at 580 nm by MB for the as-deposited MoO_{3-x} thin films on glass and FTO of 100,200,300 and 500 nm thick as a function of UV illumination time. For films deposited on glass and FTO, with increasing the irradiation time, the decomposition of the MB increases. The deposited films on glass decompose MB more than the films deposited on FTO. Besides, this decomposition of the MB seemed to decrease with increasing MoO_{3-x} film thickness from 100 to 500 nm which is in good matching with the corrosion measurements. Moreover, the as deposited MoO_{3-x} thin film

of thickness 100 nm has the greatest ability to decompose MB. This behavior is mainly attributed to the effect of the surface activity of a corresponding film. The film with low thickness provides high surface to bulk ratio compared to the high thick one [39-41].
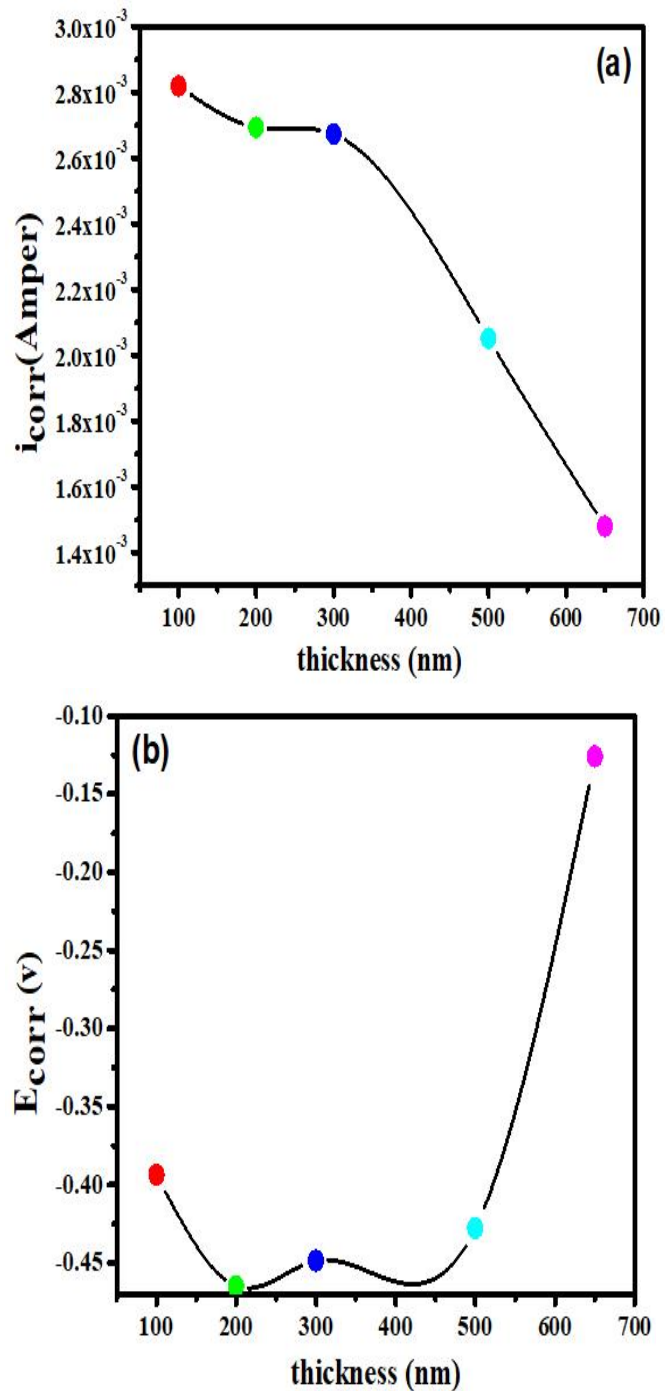

Fig.10: (a) the measured icorr values for different MoO3 film thickness, (b) the measured Ecorr values for different MoO3 film thickness.
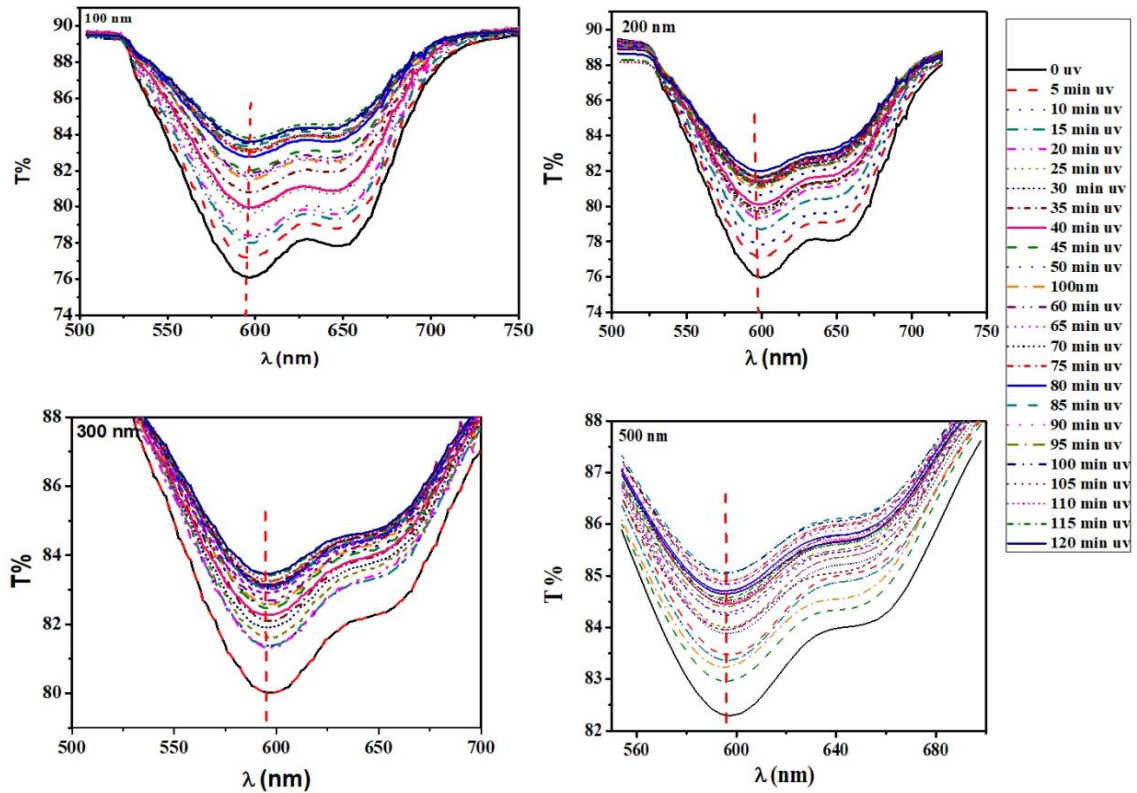
Fig.11: change of transmittance during UV illumination at different periods of time for as deposited MoO$_{3-x}$ thin films on glass substrate of 100, 200, 300 and 500nm thick.
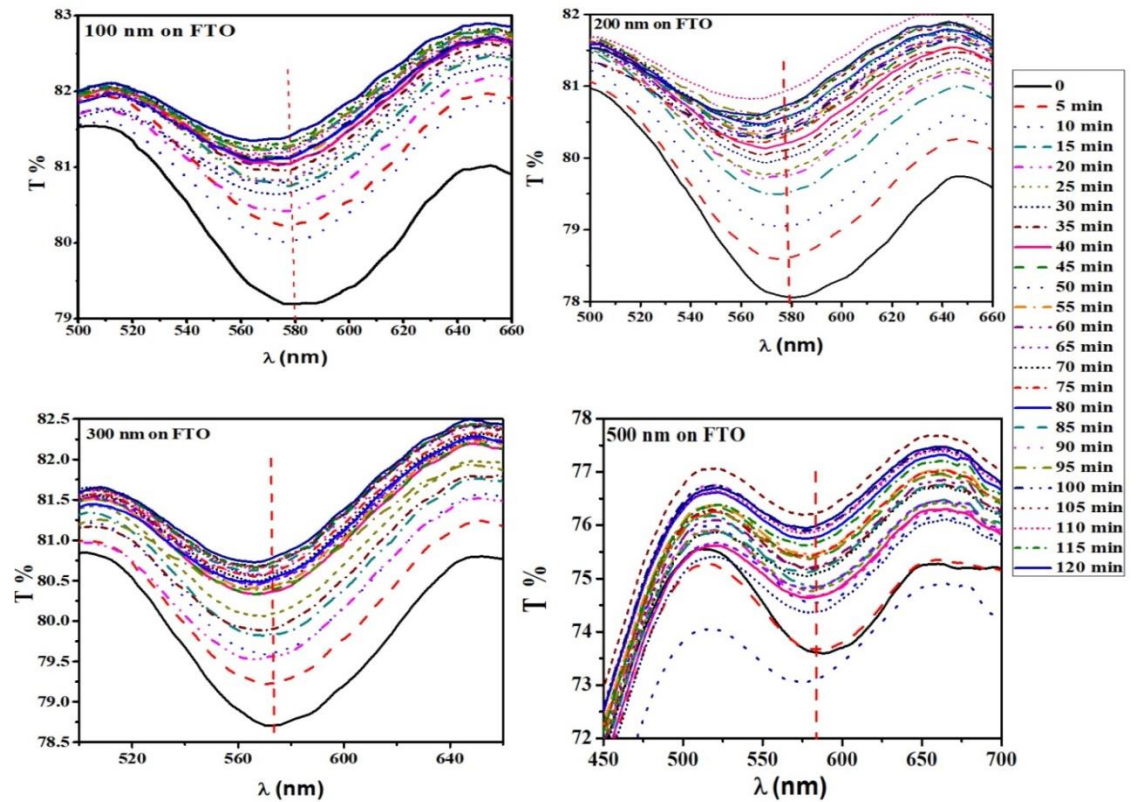

Fig.12: change of transmittance during UV illumination at different periods of time for as deposited MoO3-x thin films on FTO substrate of 100, 200, 300 and 500nm thick.
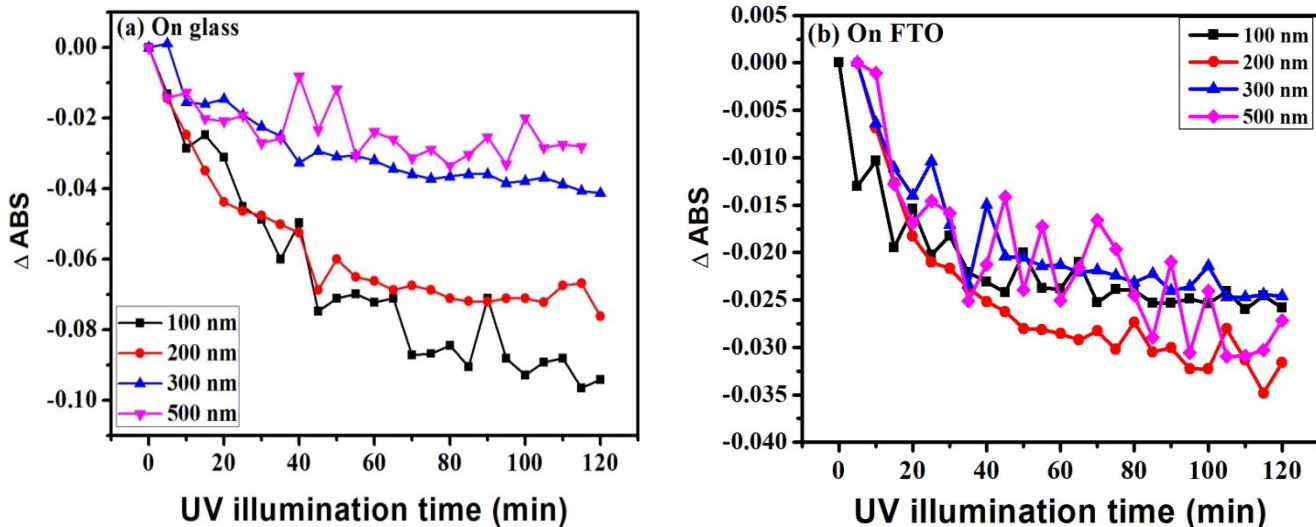
Fig.13: Variation of the absorption at 580 nm by MB as a function of illumination time for as deposited MoO3-x thin films (a)on glass, (b) on FTO.

4 Conclusions

In summary, Amorphous MoO_{3-x} thin films with different thicknesses were successfully synthesized using a simple thermal evaporation technique on glass and FTO coated glass substrates. The samples obtained were systematically characterized in detail using various standard techniques in terms of their structure, corrosion, morphology, optical and photocatalytic properties. The substrate type doesn't have a sensitive effect on the optical band gap values. The optical band gap decreases by increasing the thickness of all films, whether deposited on glass or deposited on FTO substrates and their values range from 3.1 to 3.6 eV. In addition, the Urbach energy, refractive index, extinction coefficient and dispersion energy parameters of MoO_{3-x} thin films have been determined and discussed. Corrosion measurements of the as deposited MoO_{3-x} thin film on FTO in a neutral medium of NaCl solution with concentration 3.5 g/ml revealed that the low thick films can corrode more than the high thick films.

The photocatalytic activity was evaluated by the degradation of MB. The highest photocatalytic activity was found for MoO_{3-x} films with 100 nm thick deposited on glass substrate. This result is mainly attributed to the effects of low thickness on the morphology, and surface activity of the MoO_{3-x} film.

References

[1] C. Julien, O. Mohammad Hussaxm L. E1-Farh and M. Balkanski, journal of Sohd State Ionlcs ., **53-56**, 400-40 (1992).

[2] S. Touihri , A. Arfaoui , Y. Tarchouna , A. Labidi , M. Amlouk , J.C. Bernede , journal of Applied Surface Science., **394**, 414–424 (2017).

[3] M. Kröger, S. Hamwi, J. Meyer, T. Riedl, W. Kowalsky, and A. Kahn, journal of Applied Physics Letters., **95**, 123301 (2009).

[4] S. Phadungdhitidhada , P. Mangkorntong, S. Choopun, N. Mangkorntong, journal of Ceramics International., **34,** 1121–1125 (2008).

[5] M.F. Al-Kuhaili, S.H.A. Ahmad, S.M.A. Durrani, M.M. Faiz, A. Ul-Hamid, journal of Materials and Design., **73**, 15–19 (2015).

[6] Jung Min Cho, Sang Kyu Lee, Sang-Jin Moon, Jeongdai Jo, Won Suk Shin, journal of Current Applied Physics., **14**, 1144-1148 (2014).

[7] V. K. SABHAPATHI, O.MD. HUSSAIN, P. S. REDDY, K. T. RAMAKRISHNA REDDY,S. UTHANNA, B. S. NAIDU,and P. JAYARAMA REDDY, journal of phys. stat. sol. (a) **148**, 167 (1995).

[8] R.S. Patil , M.D. Uplane , P.S. Patil , journal of Applied Surface Science 252 (2006) 8050–8056.

[9] H.M. Martı ´nez, J. Torres, M.E. Rodrı´guez-Garcı ´a, L.D. Lo ´ pez Carren ˜o, journal of Physica B., **407** 3199–3202 (2012).

[10] Yongxia Miao, Guanzhong Lu , Xiaohui Liu, Yanglong Guo, Yanqin Wang, Yun Guo, Journal of Molecular Catalysis A: Chemical., **306** 17–22 (2009).

[11] K.Galatsis , Y.X.Li , W.Wlodarski , K.Kalantar-Zadeh , journal of Sensors and Actuators B**77,** 478-483(2001).

[12] K. Khojier , H. Savaloni , S. Zolghadr , journal of Applied Surface Science., **320,** 315–321(2014).

[13] L.S. Aravinda , K.K. Nagaraja , K. Udaya Bhat , Badekai Ramachandra Bhat , Journal of Electroanalytical Chemistry., **699**, 28–32 (2013)

[14] Do Young Kim, Jegadesan Subbiah, Galileo Sarasqueta, Franky So, Huanjun Ding, Irfan, and Yongli Gao, journal of Applied Physics Letters., **95**, 093304 (2009).

[15] Mai M. Khalaf, Hany M. Abd El-Lateef and H. M. Ali, Plasmonics, 2018 https://doi.org/10.1007/s11468-018-0693-7.

[16] Phutthamon Chantes, Chalor Jarusutthirak, and Supamas Danwittayakul, journal of International Conference on Biological, Environment and Food Engineering (BEFE-2015) May 15-16, 2015 Singapore.

[17] Meshal S.Al-Johani, Yousef S.Al-Zaghayer, Sulaiman I.Al-Mayman, International Scientific Journal, Environmental Science, http://environment.scientific-journal.com.

[18] Weerachai Sangchay, journal of Advanced Materials Research ., **626**, 334-338 (2013).

[19] Sampa Chakrabarti, Binay K. Dutta, Journal of Hazardous Materials., **B112**, 269–278(2004).

[20] Takanori Mizushima , Yuri Moriya, Nguyen Huu Huy Phuc, Hironobu Ohkita, Noriyoshi Kakuta, journal of Catalysis Communications., **13,** 10–13(2011)

[21] Guojie Wang , Tonggang Jiu , Pandeng Li , Jun Li b, Chunming Sun , Fushen Lu , Junfeng Fang , journal of Organic Electronics., **15**, 29–34(2014).

[22] Feng-Kuei Chang, Yi-Chi Huang, Jiann-Shing Jeng, Jen-Sue Chen, journal of Solid-State Electronics., **122** 18–22 (2016).

[23] A.Arfaoui, S.Touihri, A.Mhamdi, A.Labidi, T.Mahoubi, journal of Applied Surface Science., **357 Part A**, 1089-1096 (2015).

[24] Liying Huang, Hui Xu, Rongxian Zhanga, Xiaonong Cheng ,Jiexiang Xia, Yuanguo Xu , HuamingLi, journal of Applied Surface Science., **283**, 25-32 (2013).

[25] Hirotaka Natori, Koichi Kobayashi and Masashi Takahashi, journal of Oleo Science., **58(4)**, (2009).

[26] Basics of Corrosion Measurements, Princeton Applied Research, 801 S. Illinois Avenue, Oak Ridge, TN 37830203-211. Tel: (865) 425-1289 Fax: (865) 481-2410 Web: www.princetonappliedresearch.com.

[27] D. R. Gabe, The centenary of Tafel's equation, journal of Transactions of the Institute of Metal Finishing., **83 (3)**, 121-124.

[28] Wei-Song Wang , Hong-Yi Huang, Shu-Chun Chen, Kuo-Chuan Ho, Chia-Yu Lin ,Tse-Chuan Chou, Chih-Hsien Hu, Wen-Fong Wang, Cheng-Feng Wu and Ching-Hsing Luo, journal of Sensors., **11**, 8593-8610.

[29] JOHN G. SIMMONS,journal of P H VSICAL REVIEW.,**155(3)**, (1967).

[30] H. Peelaers, M. L. Chabinyc, and C. G. Van de Walle, journal of Chem. Mater., **29**, 2563−2567(2017).

[31] A.A. Mane, A.V. Moholkar, Applied Surface Science., **405**, 427–440(2017).

[32] M. ANWAR and C. A. HOGARTH, jornal of phys. stat. sol. (a)109, 469 (1988) ,Subject classification: 78.65; 68.55; S10.1.

[33] Franz Urbach, journal of Phys. Rev. 92, 1324 – Published 1 December 1953.

[34] Werner Martienssen, Journal of Physics and Chemistry of Solids .,**2(4)**, 257-267(1957).

[35] H.Arifa, A.Boukhachem, B.Askri, K.Boubaker, A.Yumak, K.Raouadi, journal of Ceramics International., 2147-2157(2016).

[36] Optical properties of solids, Mark Fox, OXFORD University press, 2001.

[37] Di Domenico M., Journal of Applied Optics., **11**, 652(1972).

[38] Wemple S. H., Journal of Chemistry and Physics., **67** 2151 (1977).

[39] Chengxiang Wang, Longwei Yin , Luyuan Zhang, Dong Xiang and Rui Gao, journal of Sensors., **10**, 2088-2106(2010)

[40] Franke, M.E.; Koplin, T.J.; Simon, U. Metal and Metal Oxide Nanoparticles in Chemiresistors:Does the Nanoscale Matter? Small., **2**, 36-50(2006).

[41] Jürgen Biener, Arne Wittstock, Theodore F. Baumann, Jörg Weissmüller, Marcus Bäumer and Alex V. Hamza, journal of Materials., **2**, 2404-242(2009).